Quantum waveguide theory of Andreev spectroscopy in multiband superconductors: The case of iron pnictides

M. A. N. Araújo[1,2] and P. D. Sacramento[1]
[1]*CFIF, Instituto Superior Técnico, Universidade Técnica de Lisboa, Av. Rovisco Pais, 1049-001 Lisboa, Portugal*
[2]*Departamento de Física, Universidade de Évora, P-7000-671 Évora, Portugal*
(Received 7 January 2009; revised manuscript received 7 May 2009; published 29 May 2009)

The problem of Andreev reflection between a normal metal and a multiband superconductor is addressed. The appropriate matching conditions for the wave function at the interface are established on the basis of an extension of quantum waveguide theory to these systems. Interference effects between different bands of the superconductor manifest themselves in the conductance and the case of FeAs superconductors is specifically considered, in the framework of a recently proposed effective two-band model, in the sign-reversed *s*-wave pairing scenario. Resonant transmission through surface Andreev bound states is found as well as destructive interference effects that produce zeros in the conductance at normal incidence. Both these effects occur at nonzero bias voltage.

DOI: 10.1103/PhysRevB.79.174529 PACS number(s): 74.20.Rp, 73.20.−r, 74.50.+r, 74.70.Dd

I. INTRODUCTION

Electronic scattering at the interface between a normal metal (N) and a superconductor has been used as a probe to investigate the electronic properties of superconductors[1,2] and, more recently, FeAs superconductors (FAS), leading, in the latter case, to different conclusions regarding the pairing symmetry.[3,4] As compared to conventional and high-T_c materials, the recently discovered FeAs-based superconductors have a more complex band structure, with a Fermi surface (FS) consisting of four sheets, two of them are holelike, and the other two are electronlike.[5–8] *s*-wave, *d*-wave, and *p*-wave pairing scenarios have been proposed to describe the superconducting state.[7,9–12] One of the suggested pairing scenarios is the so-called sign-reversed *s*-wave state ($s^{\pm}$-state), where the gap function has opposite signs in the holelike and the electronlike sheets of the FS. Since this is a novel possibility, it deserves some theoretical development. A recent experiment seems to confirm this pairing scenario in a 122 compound.[13]

Blonder *et al.*[14] devised a theory for Andreev scattering in isotropic *s*-wave superconductors which has been later generalized to unconventional (anisotropic) superconductors.[15] These theories apply to one-band superconductors. In the case of multiband superconductors (MBS), such as FAS and heavy-fermion compounds, the bands are usually treated as separate conduction channels with (classically) additive conductances,[16] such as parallel resistors, thereby neglecting the quantum-mechanical nature of the scattering problem at the interface, where interference effects between the transmitted waves in different bands of the MBS are expected. Such interference effects will lead to new features in the conductance.

We are thus posed the problem of finding the wave function for the scattering state of an incident particle from a one-band metal which is transmitted through two or more bands inside the superconductor. The splitting of the incident electron's probability amplitude among several conduction channels is the same quantum-mechanical problem as in a quantum waveguide. Thus, in order to derive the appropriate matching conditions for the wave function at the interface, we need to make an extension of quantum waveguide theory.

Applying to the case of FAS, we obtain the differential conductance curves vs bias voltage and explicitly show the emergence of Andreev bound states (ABS) in the $s^{\pm}$-state scenario, as a manifestation of interference effects between the bands, unlike the usual ABS in one-band superconductors. An unusual feature of the ABS is that they occur at a finite energy above the Fermi level and disperse with the electron's transverse momentum. On the other hand, interference effects may also suppress the conductance at certain energies.

II. QUANTUM WAVEGUIDE THEORY

The splitting of the incident electron's probability amplitude among several conduction channels is the same quantum-mechanical problem as in a quantum waveguide. In a quantum waveguide, three one-dimensional conductors intercept at one point (see Fig. 1).[17] The wave function for a particle must be continuous and single-valued at the circuit node O, implying that

$$\psi(x_1 \to O) = \psi(x_2 \to O) = \psi(x_3 \to O), \tag{1}$$

where x_1, x_2, x_3 are coordinates along branches 1, 2, and 3, respectively. The (probability and charge) current conservation at the node is guaranteed by the "quantum Kirchhoff" law,[17]

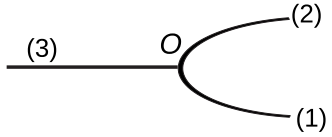

FIG. 1. Three branches of a waveguide with a node at O.

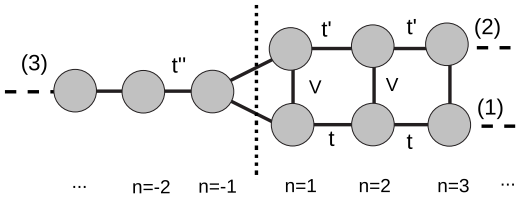

FIG. 2. Tight-binding waveguide with three branches. In branches 1 and 2 there is electron hopping along (t,t') and perpendicular (V) to the chains. An integer n labels unit cells along the chain.

$$\sum_{j=1}^{3} \frac{1}{m_j} \frac{\partial \psi(x_j \to O)}{\partial x_j} = 0, \tag{2}$$

where the coordinates $x_j (j=1,2,3)$ must be all of them directed to (or away from) the node O and m_j denotes the particle's effective mass in branch j.

A simple one-dimensional version of the N/MBS interface is a tight-binding chain which has a bifurcation at some point, as shown in Fig. 2. We further assume the sites in branch 1 to be coupled to branch 2 through a hybridization operator, $\hat{V}$. An integer n labels the two-atom unit cell along the chain.

Let $|n,j\rangle$ denote the site in cell n of chain j. Then, the incoming particle in branch 3 with wave vector p is described by the wave function $\psi_{inc}(n)=e^{ipn}+be^{-ipn}$, where b denotes the reflection amplitude.

If chains 1 and 2 were decoupled, a Bloch state in chain j would have momentum k and energy $\epsilon_j(k)$. But now suppose that an operator $\hat{V}$ hybridizes Bloch states in the two chains. The Hamiltonian matrix for the coupled chains $1+2$, $\hat{H}_{1+2}$, has an off-diagonal element, $V(k)$, and its eigenstates follow from the eigenproblem,

$$\begin{pmatrix} \epsilon_1(k) & V(k) \\ V(k) & \epsilon_2(k) \end{pmatrix} \begin{pmatrix} \alpha \\ \beta \end{pmatrix} = \mathcal{E} \begin{pmatrix} \alpha \\ \beta \end{pmatrix}, \tag{3}$$

which yields two bands, $\mathcal{E}_{\pm}(k)$, so that a Bloch state in the coupled chains $1+2$ has the form

$$\phi(n) = \begin{pmatrix} \alpha_k \\ \beta_k \end{pmatrix} e^{ikn}.$$

The eigenvector components, α and β, denote the wave-function projections on branches 1 and 2, respectively. The wave function for the transmitted particle in chains $1+2$ reads, for $n>0$,

$$\psi_t(n) = C \begin{pmatrix} \alpha_k \\ \beta_k \end{pmatrix} e^{ikn} + D \begin{pmatrix} \alpha_{k'} \\ \beta_{k'} \end{pmatrix} e^{ik'n}, \tag{4}$$

where the momenta satisfy the energy conservation condition $\mathcal{E}_-(k)=\mathcal{E}_+(k')=\epsilon(p)$. We now join the wave function in branch 3 with that in branches $1+2$ applying condition (1) and by considering that the node is reached by formally taking $n \to 0$,

$$1 + b = C\alpha_k + D\alpha_{k'} = C\beta_k + D\beta_{k'}. \tag{5}$$

In order to write Kirchhoff rule, we use the following expression for the probability current:

$$\boldsymbol{j}(\mathbf{r}) = \mathrm{Re}\{\psi^{\dagger}(\mathbf{r})(\partial \hat{H}/\partial \hat{\mathbf{k}})\psi(\mathbf{r})\}, \tag{6}$$

where the Hamiltonian is written in momentum space and the operator $\hat{\mathbf{k}}=-i\nabla$ in the continuum limit. In the tight-binding problem above, ∇ reduces to $\partial/\partial n$, and the Hamiltonian $\hat{H}$ is just the scalar dispersion $\varepsilon(\hat{p})$ in branch 3, or the Hamiltonian matrix $\hat{H}_{1+2}$ in Eq. (3) in branches $1+2$. If we write the Kirchhoff rule as the following relation between the wave functions at the circuit node:

$$\left[\frac{\partial \varepsilon}{\partial \hat{p}} \psi_{inc} \right]_{n \to 0^-} = (1,1) \cdot \left[\frac{\partial \hat{H}_{1+2}}{\partial \hat{k}} \psi_t \right]_{n \to 0^+}, \tag{7}$$

then, it can easily be checked that the current $j(n)$ is conserved at the node, by virtue of Eq. (5). The left multiplication by (1, 1) gives the sum of the currents through branches 1 and 2. Equation (7) reads

$$\frac{p}{m_n}(1-b) = C(1,1) \cdot \frac{\partial \hat{H}_{1+2}}{\partial k} \begin{pmatrix} \alpha_k \\ \beta_k \end{pmatrix} + D(1,1) \cdot \frac{\partial \hat{H}_{1+2}}{\partial k'} \begin{pmatrix} \alpha_{k'} \\ \beta_{k'} \end{pmatrix}. \tag{8}$$

where the effective mass m_n is defined as the ratio between the momentum, p, and the group velocity, $d\varepsilon(p)/dp$. The three Eqs. (5) and (8) uniquely determine the amplitudes b, C, D.

The generalization to two spatial dimensions is straightforward: the chain in Fig. 2 may be identified with the x direction and is repeated identically in the perpendicular (y) direction. The unit-cell label and momentum become two-dimensional, $\boldsymbol{n}$ and $\boldsymbol{k}$, respectively. The interface is attained as $n_x \to 0$, the transverse momentum component, k_y, is conserved. In Eq. (5) $k(k')$ is replaced by $\boldsymbol{k}(\boldsymbol{k}')$ and the Kirchhoff rule [Eq. (8)] is replaced with

$$\frac{p_x}{m_n}(1-b) = C(1,1) \cdot \frac{\partial \hat{H}_{1+2}}{\partial k_x} \begin{pmatrix} \alpha_{\mathbf{k}} \\ \beta_{\mathbf{k}} \end{pmatrix} + D(1,1) \cdot \frac{\partial \hat{H}_{1+2}}{\partial k'_x} \begin{pmatrix} \alpha_{\mathbf{k}'} \\ \beta_{\mathbf{k}'} \end{pmatrix}, \tag{9}$$

ensuring the conservation of the longitudinal current j_x at the node.

III. MODEL FOR A Fe-PNICTIDE SUPERCONDUCTOR

A recent tight-binding model[18] for the FAS band structure assumes two orbitals per unit cell, d_{xz} and d_{yz}. The Hamiltonian matrix is

$$\hat{H}(\mathbf{k}) = \begin{pmatrix} \varepsilon_x - \mu & \varepsilon_{xy} \\ \varepsilon_{xy} & \varepsilon_y - \mu \end{pmatrix}, \tag{10}$$

where μ denotes the chemical potential and

$$\varepsilon_x = -2t_1 \cos(k_x) - 2t_2 \cos(k_y) - 4t_3 \cos(k_x)\cos(k_y),$$

$$\varepsilon_y = -2t_2 \cos(k_x) - 2t_1 \cos(k_y) - 4t_3 \cos(k_x)\cos(k_y),$$

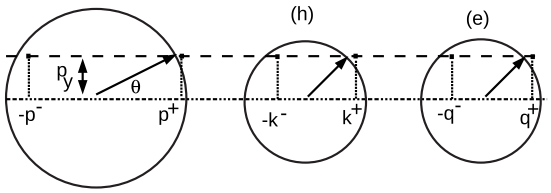

FIG. 3. Schematic representation of the Fermi surfaces of the normal metal (left), and the superconductor's h band (middle) and e band (right).

$$\varepsilon_{xy} = -4t_4 \sin(k_x)\sin(k_y). \tag{11}$$

This is analogous to branches 1 and 2 of the waveguide above, with the matrix element ε_{xy} now playing the role of the hybridization $V(\boldsymbol{k})$ between the branches 1 and 2 and $\varepsilon_{x(y)}(\boldsymbol{k})$ playing the role of $\varepsilon_{1(2)}(\boldsymbol{k})$. The parameter choice $t_1=-1$, $t_2=1.3$, $t_3=t_4=-0.85$, $\mu=1.45$ reproduces the FAS band structure.[18] In the unfolded Brillouin zone (BZ), the Fermi surface obtained from Eq. (10) has two electron pockets, centered at $(0,\pm\pi)$ and $(\pm\pi,0)$, and two hole pockets, centered at (0,0) and (π,π).

We assume the edge of the superconductor lying along the y direction. Then, an incident electron on the interface with small p_y is transmitted through two Fermi-surface pockets: the electron pocket ("e FS") and the hole pocket ("h FS"), see Fig. 3. We here work out the Andreev reflection problem in a FS consisting of just one hole and one-electron pocket. The generalization of the theory to the four pocket FS in the reduced BZ or to a model with more atoms per unit cell[3,19,20] is straightforward. We shall concentrate below on the $s^{\pm}$-state scenario for superconductivity that has recently been suggested,[7] and show that it produces ABS as a consequence of interference between transmitted waves in the two FS pockets.

An elementary excitation in the bulk superconductor with wave vector $\mathbf{k}$ has the wave function

$$\phi_{\mathbf{k}}(\mathbf{r}) = e^{i\mathbf{k}\cdot\mathbf{r}}\begin{pmatrix} u_{\mathbf{k}}\alpha_{\mathbf{k}} \\ u_{\mathbf{k}}\beta_{\mathbf{k}} \\ v_{\mathbf{k}}\alpha_{\mathbf{k}} \\ v_{\mathbf{k}}\beta_{\mathbf{k}} \end{pmatrix}, \tag{12}$$

where the coherence factors $u_{\mathbf{k}}, v_{\mathbf{k}}$, denoting the amplitudes of the particle and hole components, respectively, obey the Bogolubov–deGennes equations,[21]

$$\begin{pmatrix} \hat{H}(\mathbf{k}) & \hat{\Delta} \\ \hat{\Delta} & -\hat{H}(\mathbf{k}) \end{pmatrix}\begin{pmatrix} u_{\mathbf{k}}\alpha_{\mathbf{k}} \\ u_{\mathbf{k}}\beta_{\mathbf{k}} \\ v_{\mathbf{k}}\alpha_{\mathbf{k}} \\ v_{\mathbf{k}}\beta_{\mathbf{k}} \end{pmatrix} = \mathcal{E}\begin{pmatrix} u_{\mathbf{k}}\alpha_{\mathbf{k}} \\ u_{\mathbf{k}}\beta_{\mathbf{k}} \\ v_{\mathbf{k}}\alpha_{\mathbf{k}} \\ v_{\mathbf{k}}\beta_{\mathbf{k}} \end{pmatrix}, \tag{13}$$

with $\hat{\Delta}=\Delta(\mathbf{k})\mathrm{diag}(1,1)$. The superconducting gap $\Delta(\mathbf{k})$ is assumed to take on different values, $\Delta_h(\mathbf{k})$ and $\Delta_e(\mathbf{q})$, in the h and e FS, respectively. In the $s^{\pm}$-state scenario, $\Delta_e(\mathbf{k})$ and $\Delta_h(\mathbf{k})$ have opposite signs.[7,21]

The quasiparticle has a transverse momentum $\hbar p_y$ which is conserved. The incident particle from the normal metal has momentum $\mathbf{p}^+=\hbar(p^+,p_y)$ and the Andreev reflected hole has momentum $\mathbf{p}^-=\hbar(p^-,p_y)$. The transmitted particle (hole) in the superconductor's e band has momentum $\mathbf{q}^+=\hbar(q^+,p_y)[\mathbf{q}^-=\hbar(-q^-,p_y)]$; but the transmitted particle (hole) in the superconductor's h band has momentum $\mathbf{k}^-=\hbar(-k^-,p_y)[\mathbf{k}^+=\hbar(k^+,p_y)]$ because the effective mass, m_h, of the h FS is negative and transmitted particles/holes must have positive group velocity, see Fig. 3. The wave function for a scattering state with transverse momentum $\hbar p_y$ can be written as

$$\Psi(\mathbf{r}) = e^{ip_y y}[\psi_N(x)\theta(-x) + \psi_S(x)\theta(x)],$$

where $\theta(x)$ denotes the Heaviside function. The wave function in the normal single-band metal has both particle (u) and hole (v) components,

$$\psi_N(x<0) = \begin{pmatrix} 1 \\ 0 \end{pmatrix}e^{ip^+x} + b\begin{pmatrix} 1 \\ 0 \end{pmatrix}e^{-ip^+x} + a\begin{pmatrix} 0 \\ 1 \end{pmatrix}e^{ip^-x}, \tag{14}$$

where a is the Andreev reflection amplitude. Near the Fermi level, $p^+\approx p^-\approx p_F\sqrt{1-(p_y/p_F)^2}$, where $\hbar p_F$ denotes the Fermi momentum in the normal metal, which has Fermi velocity $v_F=\hbar p_F/m_n$. The transmitted quasiparticle into the superconductor is a linear superposition of Bloch states of the form (12) in the two bands,

$$e^{ip_y y}\psi_S(x>0) = C\phi_{\mathbf{k}^+}(\mathbf{r}) + D\phi_{\mathbf{k}^-}(\mathbf{r}) + E\phi_{\mathbf{q}^+}(\mathbf{r}) + F\phi_{\mathbf{q}^-}(\mathbf{r}). \tag{15}$$

We now apply the waveguide matching conditions, at $x=0$, between Eqs. (14) and (15), to the u and v components of the wave function, separately. The condition for the wave function to be single valued at the node reads as

$$\begin{aligned} 1+b &= Cu_{\mathbf{k}^+}\alpha_{\mathbf{k}^+} + Du_{\mathbf{k}^-}\alpha_{\mathbf{k}^-} + Eu_{\mathbf{q}^+}\alpha_{\mathbf{q}^+} + Fu_{\mathbf{q}^-}\alpha_{\mathbf{q}^-}, \\ 1+b &= Cu_{\mathbf{k}^+}\beta_{\mathbf{k}^+} + Du_{\mathbf{k}^-}\beta_{\mathbf{k}^-} + Eu_{\mathbf{q}^+}\beta_{\mathbf{q}^+} + Fu_{\mathbf{q}^-}\beta_{\mathbf{q}^-}, \\ a &= Cv_{\mathbf{k}^+}\alpha_{\mathbf{k}^+} + Dv_{\mathbf{k}^-}\alpha_{\mathbf{k}^-} + Ev_{\mathbf{q}^+}\alpha_{\mathbf{q}^+} + Fv_{\mathbf{q}^-}\alpha_{\mathbf{q}^-}, \\ a &= Cv_{\mathbf{k}^+}\beta_{\mathbf{k}^+} + Dv_{\mathbf{k}^-}\beta_{\mathbf{k}^-} + Ev_{\mathbf{q}^+}\beta_{\mathbf{q}^+} + Fv_{\mathbf{q}^-}\beta_{\mathbf{q}^-}. \end{aligned} \tag{16}$$

By solving the system [Eq. (16)] by the determinant method, the amplitudes C, D, E, F can be expressed as functions of a and b, as

$$C = \frac{(1+b)\Gamma_1 + a\Gamma_2}{\Lambda}, \tag{17}$$

$$D = \frac{(1+b)\Gamma_3 + a\Gamma_4}{\Lambda}, \tag{18}$$

$$E = \frac{(1+b)\Gamma_5 + a\Gamma_6}{\Lambda}, \tag{19}$$

$$F = \frac{(1+b)\Gamma_7 + a\Gamma_8}{\Lambda}, \tag{20}$$

where Λ is the determinant of the system [Eq. (16)] and reads

$$\Lambda = \begin{vmatrix} u_+\alpha_+ & u_-\alpha_- & u'_+\alpha'_+ & u'_-\alpha'_- \\ u_+\beta_+ & u_-\beta_- & u'_+\beta'_+ & u'_-\beta'_- \\ v_+\alpha_+ & v_-\alpha_- & v'_+\alpha'_+ & v'_-\alpha'_- \\ v_+\beta_+ & v_-\beta_- & v'_+\beta'_+ & v'_-\beta'_- \end{vmatrix}, \tag{21}$$

and the coefficients Γ_i are obtained from Cramer's rule.

We now define

$$\Theta(\mathbf{k}) = \frac{m_n}{p_+}(1,1)\cdot\left(u\frac{\partial\hat{H}}{\partial k_x} + v\frac{\partial\hat{\Delta}}{\partial k_x}\right)\begin{pmatrix}\alpha\\ \beta\end{pmatrix}, \tag{22}$$

$$\Phi(\mathbf{k}) = \frac{m_n}{p_-}(1,1)\cdot\left(v\frac{\partial\hat{H}}{\partial k_x} - u\frac{\partial\hat{\Delta}}{\partial k_x}\right)\begin{pmatrix}\alpha\\ \beta\end{pmatrix}, \tag{23}$$

and write condition (9) for this case as

$$1 - b = C\Theta(\mathbf{k}_+) + D\Theta(\mathbf{k}_-) + E\Theta(\mathbf{q}_+) + F\Theta(\mathbf{q}_-),$$

$$a = C\Phi(\mathbf{k}_+) + D\Phi(\mathbf{k}_-) + E\Phi(\mathbf{q}_+) + F\Phi(\mathbf{q}_-). \tag{24}$$

In order to simulate interface disorder, a potential barrier $U\delta(x-\epsilon)$ is assumed in the normal metal ($\epsilon<0$) and the limit $\epsilon\to 0^-$ is taken.[22] We now show that the effect of the barrier amounts to making the replacement,

$$1 - b \to 1 - b - 2iZ(1+b)p_F/p^+, \tag{25}$$

$$a \to a(1 - 2iZp_F/p^+), \tag{26}$$

on the right-hand side of Eq. (24), where the dimensionless barrier parameter[14] $Z=U/\hbar v_F$. To see this, we write the wave function in the normal single-band metal with both particle and hole components,

$$\psi_N(x \le \epsilon) = \begin{pmatrix}1\\0\end{pmatrix}e^{ip^+x} + b\begin{pmatrix}1\\0\end{pmatrix}e^{-ip^+x} + a\begin{pmatrix}0\\1\end{pmatrix}e^{ip^-x}, \tag{27}$$

and

$$\psi_N(\epsilon < x < 0) = \tilde{\alpha}\begin{pmatrix}1\\0\end{pmatrix}e^{ip^+x} + \tilde{\beta}\begin{pmatrix}1\\0\end{pmatrix}e^{-ip^+x} + \tilde{\gamma}\begin{pmatrix}0\\1\end{pmatrix}e^{ip^-x} + \tilde{\delta}\begin{pmatrix}0\\1\end{pmatrix}e^{-ip^-x}. \tag{28}$$

The matching conditions at $x=\epsilon<0$ give the equations

$$\psi_N(\epsilon^-) = \psi_N(\epsilon^+), \tag{29}$$

$$-\frac{\hbar^2}{2m_n}[\psi'_N(\epsilon^+) - \psi'_N(\epsilon^-)] + U\psi_N(\epsilon) = 0. \tag{30}$$

Taking the limit $\epsilon\to 0^-$ we obtain

$$\tilde{\alpha} + \tilde{\beta} = 1 + b, \tag{31}$$

$$\tilde{\alpha} - \tilde{\beta} = \frac{2m_nU}{i\hbar^2p^+}(1+b) + 1 - b, \tag{32}$$

$$\tilde{\gamma} + \tilde{\delta} = a, \tag{33}$$

$$\tilde{\gamma} - \tilde{\delta} = \left(\frac{2m_nU}{i\hbar^2p^-} + 1\right)a. \tag{34}$$

The waveguide matching conditions must be applied between Eqs. (28) and (15) at $x=0$. But Eqs. (31)–(34) allow the elimination of the amplitudes $\tilde{\alpha}$, $\tilde{\beta}$, $\tilde{\gamma}$, $\tilde{\delta}$ altogether, finally showing that the replacements [Eqs. (25) and (26)] have to be done in Eq. (24).

The values of the Andreev and normal reflection amplitudes, a and b, can be obtained by solving the linear system [Eqs. (16) and (24)]. Introducing

$$\zeta_{11} = \Gamma_1\Theta(\mathbf{k}_+) + \Gamma_3\Theta(\mathbf{k}_-) + \Gamma_5\Theta(\mathbf{q}_+) + \Gamma_7\Theta(\mathbf{q}_-),$$

$$\zeta_{12} = \Gamma_2\Theta(\mathbf{k}_+) + \Gamma_4\Theta(\mathbf{k}_-) + \Gamma_6\Theta(\mathbf{q}_+) + \Gamma_8\Theta(\mathbf{q}_-),$$

$$\zeta_{21} = \Gamma_1\Phi(\mathbf{k}_+) + \Gamma_3\Phi(\mathbf{k}_-) + \Gamma_5\Phi(\mathbf{q}_+) + \Gamma_7\Phi(\mathbf{q}_-),$$

$$\zeta_{22} = \Gamma_2\Phi(\mathbf{k}_+) + \Gamma_4\Phi(\mathbf{k}_-) + \Gamma_6\Phi(\mathbf{q}_+) + \Gamma_8\Phi(\mathbf{q}_-), \tag{35}$$

we obtain

$$a = \frac{2\zeta_{21}/\Lambda}{\left(1 + 2iZ + \frac{\zeta_{11}}{\Lambda}\right)\left(1 - 2iZ - \frac{\zeta_{22}}{\Lambda}\right) + \frac{\zeta_{12}\zeta_{21}}{\Lambda^2}}, \tag{36}$$

and

$$b = \frac{\left(1 - 2iZ - \frac{\zeta_{11}}{\Lambda}\right)\left(1 - 2iZ - \frac{\zeta_{22}}{\Lambda}\right) - \frac{\zeta_{12}\zeta_{21}}{\Lambda^2}}{\left(1 + 2iZ + \frac{\zeta_{11}}{\Lambda}\right)\left(1 - 2iZ - \frac{\zeta_{22}}{\Lambda}\right) + \frac{\zeta_{12}\zeta_{21}}{\Lambda^2}}. \tag{37}$$

The contribution of this scattering state to the differential conductance is given by

$$g_s = 1 + |a|^2 - |b|^2. \tag{38}$$

The normal-state conductance, $g_n=1-|b_n|^2$, is obtained when $\Delta(\mathbf{k})=0$. Experimentally, the integral of g_s (or g_n) over the transverse momenta of the incident electrons, $\sigma_S = \int g_s dp_y$ (or $\sigma_N=\int g_n dp_y$) is measured.[15] We define the integrated relative differential conductance as σ_S/σ_N.

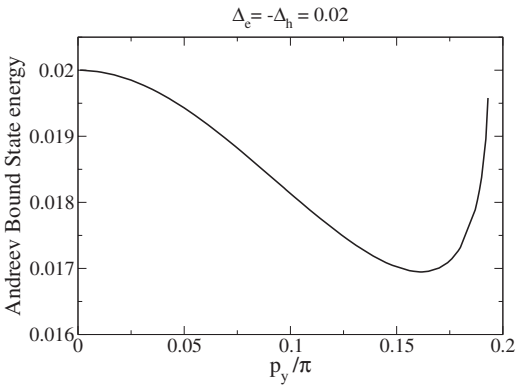

FIG. 4. Energy of the surface Andreev bound state as function of the transverse momentum. $\Delta_e=-\Delta_h=0.02$.

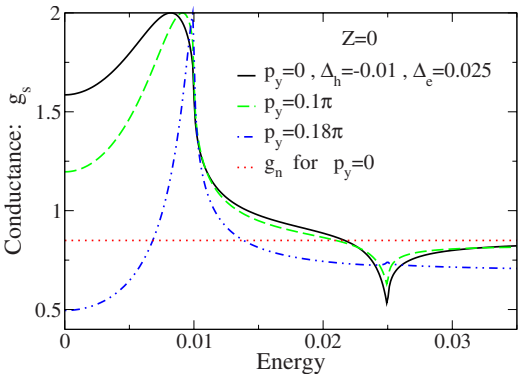

FIG. 5. (Color online) Conductance g_s as function of incident electron energy for three different values of the transverse momentum, for a clean ($Z=0$) interface. The superconductor bands are modeled by Eqs. (10) and (11). The normal conductance is shown for comparison.

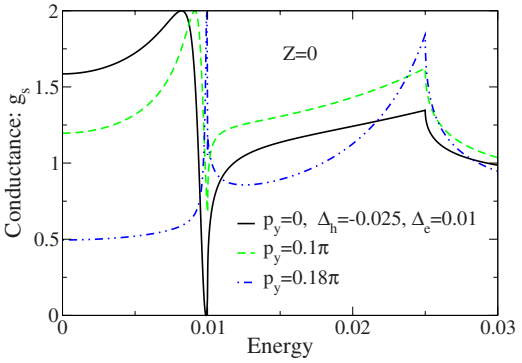

FIG. 6. (Color online) Conductance g_s as function of incident electron energy for three different values of the transverse momentum, for a clean ($Z=0$) interface. $\Delta_e=0.01, \Delta_h=-0.025$.

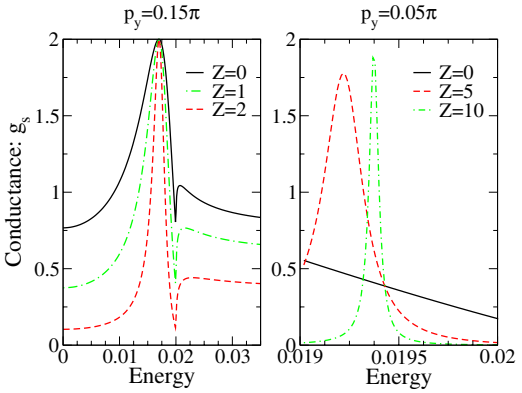

FIG. 7. (Color online) The conductance g_s is independent of the barrier strength, Z, at the energy of the ABS. The latter can be checked from Fig. 4. This is shown for two transverse momenta: $p_y=0.15\pi$ (left); $p_y=0.05\pi$ (right). $\Delta_e=-\Delta_h=0.02$.

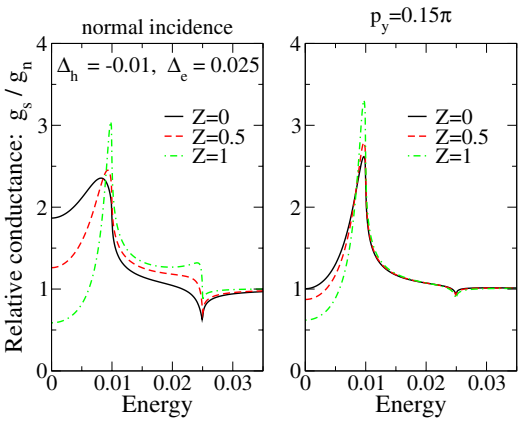

FIG. 8. (Color online) Relative conductance g_s/g_n for a disordered interface, at two different values of transverse momentum. $\Delta_h=-0.01, \Delta_e=0.025$.

IV. RESULTS

The conductances σ_S and $g_s(\mathcal{E})$ have been calculated from the above theory using the model [Eqs. (10) and (11)]. We discuss the results below. In the calculations, the normal metal is assumed to have Fermi wave vector $p_F=\pi$ and velocity $v_F=1.83$.

When $\Lambda=0$ the reflection amplitudes, hence g_s, become independent of the barrier parameter Z and this is precisely the condition for the occurrence of Andreev bound states.[15,23,24] Figure 4 shows the energy of the Andreev bound state as function of the transverse momentum. Contrary to the usual case of single-band nonconventional superconductors, the ABS energy is nonzero. It has a nonmonotonic dependence on p_y and, for $p_y=0$, it coincides with $\min(|\Delta_h|,|\Delta_e|)$. The dispersion of the ABS energy is in qualitative agreement with the results of Ref. 25.

Figure 5 shows the conductance g_s as function of incident electron energy above the Fermi level, for a clean ($Z=0$) interface in the case where $|\Delta_h|<|\Delta_e|$. When the transverse momentum increases, g_s becomes more strongly peaked near the energy of the ABS. In the case where $|\Delta_h|>|\Delta_e|$ there is a destructive interference effect leading to a zero, at normal

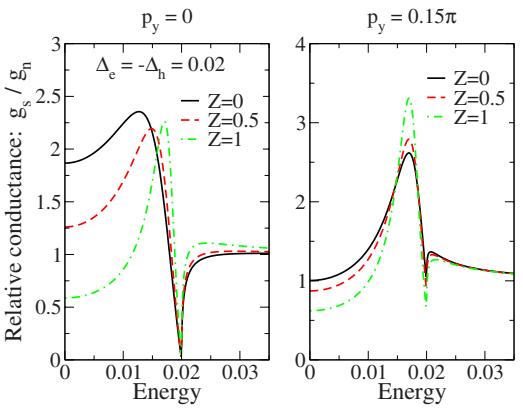

FIG. 9. (Color online) Behavior of the relative conductance for different disorder values, Z. Destructive interference effects cause a zero in the conductance. $\Delta_e=-\Delta_h=0.02$.

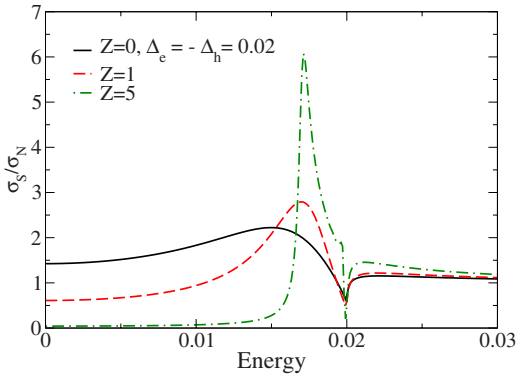

FIG. 10. (Color online) Behavior of the integrated relative differential conductance, σ_S/σ_N, for different disorder values, Z. $\Delta_e=-\Delta_h=0.02$.

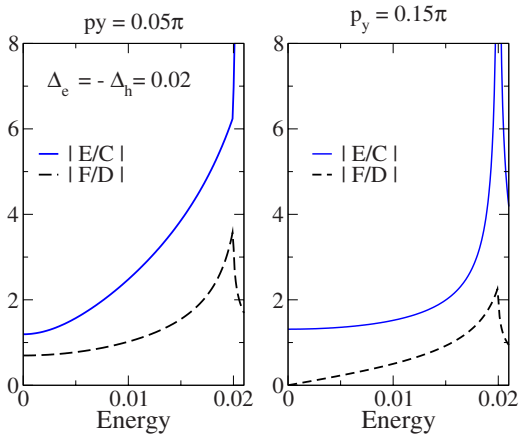

FIG. 11. (Color online) The ratio of the moduli of amplitudes $|E/C|$ and $|F/D|$ as a function of energy. The transverse momentum $p_y=0.05\pi$ (left panel) and $p_y=0.15\pi$ (right panel). $\Delta_e=-\Delta_h=0.02$.

incidence, in the conductance, as shown in Fig. 6.

The effect of interface disorder is shown in Figs. 7–9. Under increasing disorder, conductance peaks appear closer to the energy of ABS. The conductance g_s is independent of the disorder parameter, Z, at the ABS energy, therefore, all the conductance curves $g_s(E)$, for different Z values, intercept at the same point, as shown in Fig. 7. As disorder increases the conductance tends to decrease and, therefore, the normal-state conductance decreases as Z increases. Since at the ABS the conductance g_s is independent of the disorder parameter, Z, peaks appear in the relative conductance at the ABS, which become more pronounced as Z gets larger. The relative conductance g_s/g_n is plotted for two ratios of the gap parameters in Figs. 8 and 9, illustrating the positions of the peaks. The case when $\Delta_h=-\Delta_e$ is shown in Fig. 9. It is also seen, once again, that destructive interference effects in the superconductor between the e and h bands cause the conductance to vanish at normal incidence.

Since the system is two-dimensional we have to integrate over the possible incident angles, or over p_y. The integrated relative conductance is shown in Fig. 10 for three interface disorder strengths. The peak structure for large values of the barrier strength reveals the existence of ABS.

In a recent preprint,[23] a theory is provided that qualitatively predicts the interference effects in the multiband superconductor, namely, the suppression of conductance and the appearance of ABS, in agreement with our findings. In Ref. 23, the wave function in the superconductor is written in the same form as Eq. (15) but it is assumed that the ratios of the amplitudes E/C and F/D are equal (to a phenomenological parameter α introduced in Ref. 23). Using our waveguide theory for the interface matching conditions, we find that the ratios E/C and F/D are different, as can be seen from Fig. 11.

V. SUMMARY

We have introduced a generalization of the quantum waveguide theory to determine the appropriate boundary conditions for the wave function at the interface between a normal metal and a multiband superconductor. We have shown that resonant transmission and destructive interference effects occur in the sign-reversed scenario for pnictide superconductors. Unlike other unconventional superconductors, Andreev bound states at finite energies are brought about by these interference effects.

On the experimental side, polycrystalline samples have been used so far. The results obtained above describe an interface parallel to the nearest Fe-Fe bonding. Therefore, experiments with single crystals are highly desirable. If the edge of the sample is such that the conservation of the transverse momentum p_y intercepts only one FS pocket, existing one-band theories apply. The above quantum waveguide theory can in principle be used to describe other MBS, such as the heavy-fermion materials.[22]

ACKNOWLEDGMENTS

We would like to thank Vítor R. Vieira for a discussion and comments on the paper.

[1] M. Tinkham, *Introduction to Superconductivity*, 2nd ed. (Dover Publications, New York, 2004).
[2] W. K. Park, L. H. Greene, J. L. Sarrao, and J. D. Thompson, Phys. Rev. B **72**, 052509 (2005).
[3] T. Y. Chen, Z. Tesanovic, R. H. Liu, X. H. Chen, and C. L. Chien, Nature (London) **453**, 1224 (2008).
[4] Y.-L. Wang, L. Shan, L. Fang, P. Cheng, C. Ren, and H.-H. Wen, Supercond. Sci. Technol. **22**, 015018 (2009).
[5] D. J. Singh and M.-H. Du, Phys. Rev. Lett. **100**, 237003 (2008).
[6] G. Xu, W. Ming, Y. Yao, X. Dai, S.-C. Zhang, and Z. Fang, Europhys. Lett. **82**, 67002 (2008).
[7] I. I. Mazin, D. J. Singh, M. D. Johannes, and M. H. Du, Phys.

Rev. Lett. **101**, 057003 (2008); V. Cvetkovic and Z. Tesanovic, Europhys. Lett. **85**, 37002 (2009).
[8] K. Haule, J. H. Shim, and G. Kotliar, Phys. Rev. Lett. **100**, 226402 (2008).
[9] A. V. Chubukov, D. V. Efremov, and I. Eremin, Phys. Rev. B **78**, 134512 (2008).
[10] X.-L. Qi, S. Raghu, Chao-Xing Liu, D. J. Scalapino, and Shou-Cheng Zhang, arXiv:0804.4332 (unpublished).
[11] P. A. Lee and X. G. Wen, Phys. Rev. B **78**, 144517 (2008).
[12] Z.-J. Yao, Jian-Xin Li, and Z. D. Wang, New J. Phys. **11**, 025009 (2009).
[13] A. D. Christianson, E. A. Goremychkin, R. Osborn, S. Rosenkranz, M. D. Lumsden, C. D. Malliakas, I. S. Todorov, H. Claus, D. Y. Chung, M. G. Kanatzidis, R. I. Bewley, and T. Guidi, Nature (London) **456**, 930 (2008).
[14] G. E. Blonder, M. Tinkham, and T. M. Klapwijk, Phys. Rev. B **25**, 4515 (1982).
[15] S. Kashiwaya, Y. Tanaka, M. Koyanagi, and K. Kajimura, Phys. Rev. B **53**, 2667 (1996).
[16] J. Linder and A. Sudbo, Phys. Rev B **79** 020501(R) (2009).
[17] J.-B. Xia, Phys. Rev. B **45**, 3593 (1992).
[18] S. Raghu, Xiao-Liang Qi, Chao-Xing Liu, D. J. Scalapino, and Shou-Cheng Zhang, Phys. Rev B **77**, 220503(R) (2008).
[19] C. Cao, P. J. Hirschfeld, and H. P. Cheng, Phys. Rev. B **77**, 220506(R) (2008).
[20] K. Kuroki, Seiichiro Onari, Ryotaro Arita, Hidetomo Usui, Yukio Tanaka, Hiroshi Kontani, and Hideo Aoki, Phys. Rev. Lett. **101**, 087004 (2008).
[21] Y. Bang and H.-Y. Choi, Phys. Rev. B **78**, 134523 (2008).
[22] M. A. N. Araújo and P. D. Sacramento, Phys. Rev. B **77**, 134519 (2008).
[23] A. A. Golubov, A. Brinkman, O. V. Dolgov, I. I. Mazin, and Y. Tanaka, arXiv:0812.5057 (unpublished).
[24] The limit $\Lambda \rightarrow 0$ leads to zeros in the parameters ζ_{ij}. L'Hôpital's rule must be observed while taking limit $\Lambda \rightarrow 0$ in Eqs. (36) and (37).
[25] P. Ghaemi, F. Wang, and A. Vishwanath, Phys. Rev. Lett. **102**, 157002 (2009).